# Mixed layer depth variability over the global ocean

A. Birol Kara

Center for Ocean-Atmospheric Prediction Studies, Florida State University, Tallahassee, Florida, USA

Peter A. Rochford and Harley E. Hurlburt

Oceanography Division, Naval Research Laboratory, Stennis Space Center, Mississippi, USA

[1]   The spatial and monthly variability of the climatological mixed layer depth (MLD) for the global ocean is examined using the recently developed Naval Research Laboratory (NRL) Ocean Mixed Layer Depth (NMLD) climatologies. The MLD fields are constructed using the subsurface temperature and salinity data from the World Ocean Atlas 1994 [*Levitus et al.*, 1994; *Levitus and Boyer*, 1994]. To minimize the limitations of these global data in the MLD determination, a simple mixing scheme is introduced to form a stable water column. Using these new data sets, global MLD characteristics are produced on the basis of an optimal definition that employs a density-based criterion having a fixed temperature difference of $\Delta T = 0.8°C$ and variable salinity. Strong seasonality of MLD is found in the subtropical Pacific Ocean and at high latitudes, as well as a very deep mixed layer in the North Atlantic Ocean in winter and a very shallow mixed layer in the Antarctic in all months. Using the climatological monthly MLD and isothermal layer depth (ILD) fields from the NMLD climatologies, an annual mean $\Delta T$ field is presented, providing criteria for determining an ILD that is approximately equivalent to the optimal MLD. This enables MLD to be determined in cases where salinity data are not available. The validity of the correspondence between ILD and MLD is demonstrated using daily averaged subsurface temperature and salinity from two moorings: a Tropical Atmosphere Ocean array mooring in the western equatorial Pacific warm pool, where salinity stratification is important, and a Woods Hole Oceanographic Institute (WHOI) mooring in the Arabian Sea, where strongly reversing seasonal monsoon winds prevail. In the western equatorial Pacific warm pool the use of ILD criterion with an annual mean $\Delta T$ value of $0.3°C$ yields comparable results with the optimal MLD, while large $\Delta T$ values yield an overestimated MLD. An analysis of ILD and MLD in the WHOI mooring show that use of an incorrect $\Delta T$ criterion for the ILD may underestimate or overestimate the optimal MLD. Finally, use of the spatial annual mean $\Delta T$ values constructed from the NMLD climatologies can be used to estimate the optimal MLD from only subsurface temperature data via an equivalent ILD for any location over the global ocean.     *INDEX TERMS:* 4227 Oceanography: General: Diurnal, seasonal, and annual cycles; 4568 Oceanography: Physical: Turbulence, diffusion, and mixing processes; 4572 Oceanography: Physical: Upper ocean processes; 4599 Oceanography: Physical: General or miscellaneous; *KEYWORDS:* mixed layer, isothermal layer, seasonal cycle, temperature, salinity, verification

## 1.  Introduction

[2]   Ocean mixed layer depth (MLD) is one of the most important quantities of the upper ocean because it defines the quasi-homogeneous surface region of density that directly interacts with the atmosphere. For example it is significant in determining the volume or mass over which the net surface heat flux comes to be distributed [*Chen et al.*, 1994], near surface acoustic propagation [*Sutton et al.*, 1993], and ocean biology [*Polovina et al.*, 1995; *Fasham*, 1995]. As commonly known, ocean MLD is primarily determined by the action of turbulent mixing of the water mass due to wind stress and heat exchange at the air-sea interface. Turbulent mixing is predominantly the result of stirring by turbulent eddies and is most pronounced along isopycnal surfaces where it may occur with the least expenditure of energy. It is a fully three-dimensional physical process that leads to the formation of an observed uniform surface region of density (or temperature) that is generally interpreted as the ocean mixed layer. To simplify interpretation, a boundary is commonly defined to delineate the extent of the turbulent

mixed layer, namely the MLD, and the variability of the mixed layer is studied in terms of this quantity.

[3] Ocean MLD variability is not as well understood or observed as the atmospheric boundary layer. There are a few reasons for this state of affairs. One reason is the lack of temperature and salinity data with depth in some regions of the global ocean. Another is that understanding the spatial and temporal variability of the ocean mixed layer has been difficult because of the many different definitions used in the literature that are based on a temperature-based criterion, i.e., an isothermal layer depth (ILD) [e.g., *Obata et al.*, 1996], or a density-based criterion that includes the effects of salinity, i.e., a MLD [e.g., *Lewis et al.*, 1990]. Furthermore, while the ILD is generally coincident with the MLD over most of the global ocean because of the presence of a strong thermocline, there are regions such as the western equatorial Pacific and southern latitudes where there are large differences between the ILD and MLD. For this reason, studies based on an ILD determination may not be truly representative of the turbulence generated mixed layer. This lack of suitable observational data in combination with an improper definition of MLD may therefore yield misleading information on the spatial and temporal variability of the surface mixed layer. This can adversely affect ocean models that often tune their turbulent physics to reproduce the observed MLD variability, thereby yielding incorrect predictions on the upper ocean processes that are modeled.

[4] MLD fields determined for specific regions of the global ocean have been published. For example, *Bathen* [1972] examined MLD characteristics in the Pacific Ocean, *Sprintall and Tomczak* [1992] and *You* [1995] studied barrier layer formation with respect to ILD and MLD in the equatorial ocean, and the formation of a barrier layer in the western equatorial Atlantic was explained by *Pailler et al.* [1999]. However, with some limitations there are only a few studies that discuss MLD fields for the global ocean. For example, *Levitus* [1982] did not explicitly account for salinity factors in arriving at global MLD fields, while *Monterey and Levitus* [1997] extended that study with one ILD and two MLD definitions. *Monterey and Levitus* [1997] defined the ILD using a fixed temperature criterion of 0.5°C. One of the MLD was defined using a fixed density criterion of $0.125\sigma_t$, while the other MLD was defined using a variable $\Delta\rho$ criterion for a 0.5°C temperature change based on the temperature dependence of the thermal expansion of surface seawater. Of these two MLD definitions, only the latter takes account of the spatial variations in density with water properties.

[5] To address this state of affairs we construct new global MLD and ILD climatologies that provide an optimal representation of the depth of the turbulent mixed layer, and use them to describe and discuss the monthly variability of the mixed layer over the global ocean. These climatologies meet a particular need of ocean modelers to have global MLD fields that can be used for validation of ocean general circulation models (OGCMs) with an embedded mixed layer [e.g., *Cherniawsky and Holloway*, 1991]. They are also a helpful aid to model development, because of the need to parameterize in an OGCM the physics of the upper ocean structure. The climatologies are constructed using a methodology for an optimal definition of ocean MLD and ILD that was presented and evaluated in a previous study

[*Kara et al.*, 2000a]. In this paper we extend the ILD and MLD analysis over the global ocean, and describe the methods applied to handle data limitations when determining MLD over sparse data regions. We also exploit the availability of these monthly climatologies to ascertain a temperature difference ($\Delta T$) field from which an ILD can be determined that is approximately equivalent to a MLD obtained using our optimal definition. We have already shown that these MLD and ILD climatologies are useful for investigating barrier layers in the equatorial Pacific and subpolar North Pacific [*Kara et al.*, 2000b], but limited our discussion to the equatorial and North Pacific.

[6] In section 2 the temperature and salinity data used for constructing the global ocean MLD fields are described. Section 3 summarizes the MLD criterion that accounts for salinity changes. The monthly variability of the climatological MLD fields over the global ocean are introduced in section 4, followed by a discussion concerning ILD and MLD relationship in section 5. Section 6 presents a validation of the ILD versus MLD correspondence using daily subsurface temperature and salinity data from 2 moorings. Conclusions are given in section 7.

## 2. Data and Limitations

[7] To obtain global MLD fields, monthly averaged temperature and salinity profiles are used from the World Ocean Atlas provided by *Levitus et al.* [1994] and *Levitus and Boyer* [1994]. This data set will be referred to as the Levitus data throughout the remainder of the paper. The Levitus data are defined at fixed depth levels of 0, 10, 20, 30, 50, 75, 100, 125, 150 m, every 50 m to 300 m, and then every 100 m to a depth of 1000 m. We calculate the density at the Levitus levels using the standard United Nations Educational, Scientific, and Cultural Organization (UNESCO) equation of state with no pressure dependence, i.e., zero pressure [*Millero et al.*, 1980; *Millero and Poisson*, 1981]. The use of a pressure dependent equation of state yields a MLD that is inconsistent with the ILD inferred from the temperature profiles [*Kara et al.*, 2000a]. It is worthwhile to note that the surface ocean layer depth determination is affected by significant biases in the Levitus temperature, salinity and calculated density profiles that arise due to the method and sparsity of in situ sampling. As will be explained later, we process the Levitus climatology fields to remove possible biases in the data set for this study.

[8] There are limitations to the Levitus data. While there is dense data coverage for temperature and salinity over most regions of the global ocean (e.g., the North Atlantic [*Bretherton et al.*, 1984], the North Pacific [*Tabata and Weichselbaumer*, 1992], and the equatorial ocean [*Hayes et al.*, 1991; *McPhaden*, 1995]), the data coverage in the Southern Ocean still remains poor south of 30°S [*Colossi and Barnett*, 1990]. Even though the World Ocean Circulation Experiment (WOCE) has improved the quality of the temperature and salinity data in the Southern Ocean since 1990 [e.g., *Festa and Molinari*, 1992; *Gouretski*, 1999], these data were not included in the Levitus data, and the problem remains of resolving the seasonal cycle in the Southern Ocean because of the strong bias of the data density to the austral summer [*Olbers et al.*, 1992]. As a consequence, one must overcome
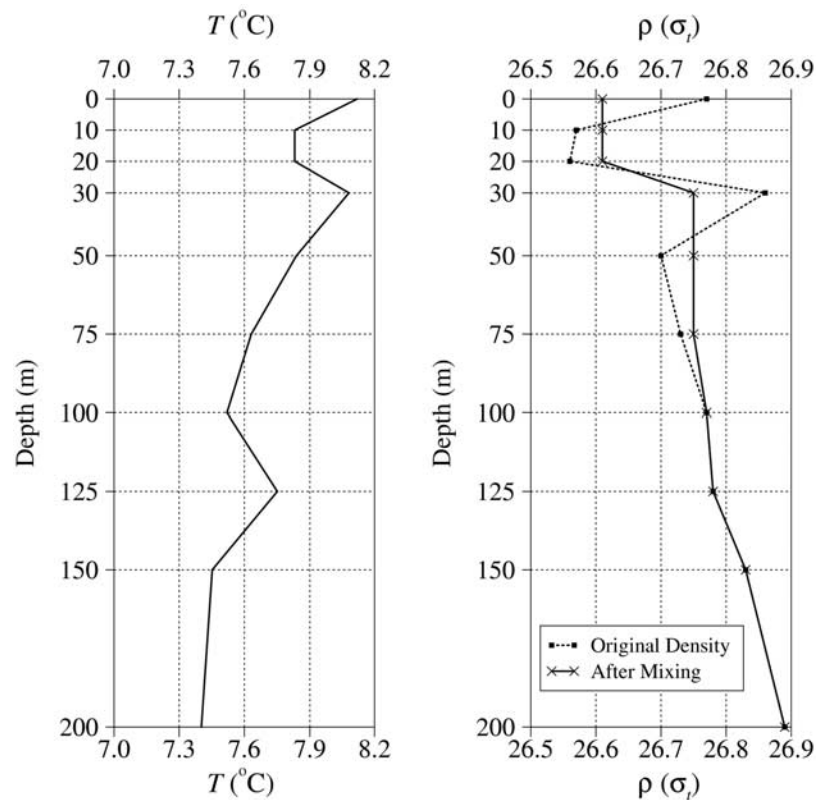
**Figure 1.** A schematic illustration of the convective mixing scheme applied to the density profiles to ensure stability. The temperature and density profiles shown are at (45°S, 60°E) in the Southern Ocean for December. Mixing is applied at the Levitus depth levels proceeding from the ocean bottom to the surface using a simple mass exchange to stabilize the water column.

the problem of deficiencies in the Levitus data for the Southern Ocean when determining the MLD.

[9] One of the difficulties with the profiles used for the Levitus climatologies is the merging of temperature and salinity data taken with a CTD (Conductivity Temperature Depth) sensor in the upper 500 m with that from an XBT (expendable bathythermograph) at greater depth. This can lead to false vertical gradients in the profiles because of changes in the quantity of temperature and salinity data as a function of depth. In general, variations in maximum depth of measurement are a serious problem because many XBTs stop at 400 m while others at 800 m. The sparsity of sampling can also provide a misleading indication of the climatological state of the ocean. Individual profiles can capture short-term dynamic processes such as eddies or the interleaving of a temperature front where multiple temperature inversions occur with depth in the upper ocean. When a small number of such profiles are used for a climatology in a data sparse region, such as the Southern Ocean, one obtains a misleading nonequilibrium representation of the ocean temperature and salinity [e.g., *Saunders*, 1986]. In addition to these limitations, temperature and salinity data obtained from ships and buoys are also subject to systematic differences in the number of observations, and are dominated by observations from one platform type or another within different gridded latitude-longitude boxes for this data set. This is a long known bias common to many climatological data sets [e.g., *Woodruff et al.*, 1987; *Wilkerson and Earle*, 1990; *Kent et al.*, 1993].

[10] As noted by *Levitus and Boyer* [1994] there could be two or more density inversions (or instabilities) in their standard level profiles. This occurs because a profile might be an average of only a handful of observations with differing maximum depths or because it is dominated by data from a single short observation period. Such multiple inversions are common in the Southern Ocean (Figure 1). Although stability checks were performed on observed as well as standard levels in the Levitus data no significant correction was applied to these kinds of profiles. The presence of these unrealistic inversions strongly affects the determined MLD. Rejection of the suspect data profiles introduces data voids over large regions of the Southern Ocean and makes construction of the ILD and MLD fields for this region difficult. Methods such as optimal interpolation would produce ILD and MLD values for this region that are very suspect. To overcome this problem we therefore choose to use a simple convective mixing scheme to remove such instabilities from the density profiles. By modifying the original data in such a manner a more realistic MLD is obtained for the suspect data profiles tested and does not introduce artificial mixed layers. A better determination of the mixed layer in the Southern Ocean awaits the availability of more temperature and salinity data.

[11] The scheme we apply searches the density profile from the ocean bottom to the surface for a density instability. When the density of a Levitus level $i$ is found to be greater than the density of its adjacent level below $i + 1$ (e.g., the density at 30 m is larger than that at 50 m) the water masses

of the two levels are mixed so they are the same density. The water masses are calculated by multiplying the density of a Levitus level $\rho_i$ by the depth range $\Delta z_i$ for that level. The latter is the distance between the midpoints to the adjacent levels $\Delta z_i = (z_{i-1} - z_{i+1})/2$, where $z_{i-1}$ and $z_{i+1}$ are depths of the adjacent levels $i - 1$ and $i + 1$, respectively. The sum of the water masses at the two levels is then averaged over their combined depth range to obtain a new density

$$\bar{\rho} = \frac{(\Delta z_i \rho_i + \Delta z_{i+1} \rho_{i+1})}{(\Delta z_i + \Delta z_{i+1})}$$

that is assigned as the density of both levels. The profile is then searched again from the bottom for a density instability and the same mixing scheme applied for all density instabilities encountered. This process is repeated until a stable density profile is produced throughout the water column.

## 3. Mixed Layer Processes and MLD Criterion

[12] While the mixed layer (isothermal layer) in its simplest conceptual form is a homogenous surface layer of density (temperature), the occurrence of other intervening physical processes can alter this simple picture. For example, after a deepening of the mixed layer due to a period of sustained increased winds or surface cooling, the density of the water column will become restratified thereby producing secondary pycnoclines or fossil layers. This occurs because the depth of turbulent mixing has shallowed in response to the weakening winds and/or increase in surface heating, beginning the formation of a new shallower mixed layer that overlies a uniformly mixed region of water mass formed from the earlier deepening event. Another example is the interleaving of water mass due to the intrusion of a front, or a jet of sinking colder water, that distorts the vertical structure of the homogenous density or temperature layer. These distortions that are instantaneously measured by XBTs typically become vertically mixed by the action of turbulence over timescales of minutes to a few hours to finally reproduce the mixed layer.

[13] In all cases, the mixed layer is a consequence of the full three-dimensional turbulence that is acting continuously on the water column as a consequence of the forcing at the ocean surface, and in the presence of horizontal processes such as lateral advection. Any criterion applied to define the mixed layer must be sufficiently robust to accommodate these many possibilities. The MLD (ILD) criterion must also be based on the variation of the density (temperature) with depth to fully account for all intervening horizontal and vertical processes. Finally, the choice of in situ property to be used for defining the MLD must be guided by turbulence theory if it is to be representative of the depth of turbulent mixing.

[14] Turbulence considerations dictate that density stratification with depth be used to define the MLD. The amount of energy available for turbulent mixing is quantitatively defined in terms of the available turbulent kinetic energy [*Kundu*, 1990]. Under the good assumption of horizontal homogeneity, the turbulent kinetic energy available in the upper ocean can be estimated in a bulk mixed layer model from the wind stress, heat flux, and freshwater flux at the air-sea interface in combination with the model MLD [e.g., *Kraus and Turner*, 1967]. Whenever the

available turbulent kinetic energy is positive, implying the turbulence at depth is greater than the latest model MLD, water mass is entrained into the mixed layer until the kinetic energy is converted into increased potential energy of the water column. The density stratification at the onset, and its subsequent modification upon entraining water into the surface layer, controls the depth of the turbulent mixing. Whenever the available turbulent kinetic energy is negative, turbulent mixing is suppressed and the uniformly mixed layer of density will become restratified as a function of other intervening physical processes as described above.

[15] The extent to which there is turbulent mixing, and hence the magnitude of the eddy viscosity for horizontal and vertical advection, depends upon the density stratification of the water column [e.g., *Pickard and Emery*, 1990]. If the water column is well mixed and hence very homogeneous, the density will vary little with depth, and turbulent mixing will easily overturn the water column. If the water column is well stratified so that density increases relatively sharply with depth, then the situation is stable and turbulent mixing is suppressed. In all cases the approximately uniform region of density provides the best indication of the mixed layer.

[16] Note that the ILD and MLD will not be the same in general. The heat and freshwater fluxes that combine to produce the buoyancy contribution in the turbulent kinetic energy act independently upon the temperature and salinity of the water column, respectively. Under conditions where surface freshwater fluxes are considerable, or where strong surface cooling has deepened the thermocline to where salinity stratification becomes important, one fully expects the surface layers for density, temperature, and salinity to each differ in depth. A notable example is a barrier layer, which is defined to be the layer of water between the MLD and ILD that forms whenever the MLD is shallower than the ILD. Barrier layers form in the western equatorial Pacific Ocean [e.g., *Vialard and Delecluse*, 1998] and western tropical Atlantic Ocean [e.g., *Pailler et al.*, 1999] because surface freshwater fluxes produce shallow and strong haloclines. Another example is the seasonal formation of the barrier layer in the North Pacific where strong surface cooling in winter increases the ILD to below the halocline so that salinity stratification produces a shallower MLD than ILD [*Kara et al.*, 2000b].

[17] Even in the absence of vertical turbulent mixing, heat and salt diffuse through seawater as a result of processes occurring at the molecular level. The upper part of the water column loses heat to the lower part while salt is gained by the upper water column at the expense of the lower. Heat loss occurs much more rapidly than salt gain in the upper water column because the rate of molecular diffusion for heat is much larger than that for salt. The density of the upper water column increases and tends to sink, while the lower water column becomes less dense and tends to rise, thereby producing a uniform layer via this double diffusion. This process occurs whenever the two interfaces are present and eventually develops homogeneous density layers with sharply defined interfaces. Thus, even when there is no turbulent mixing the ILD and MLD will not coincide because of double diffusion.

[18] Our global MLD fields are determined using the monthly averaged temperature and density data described in
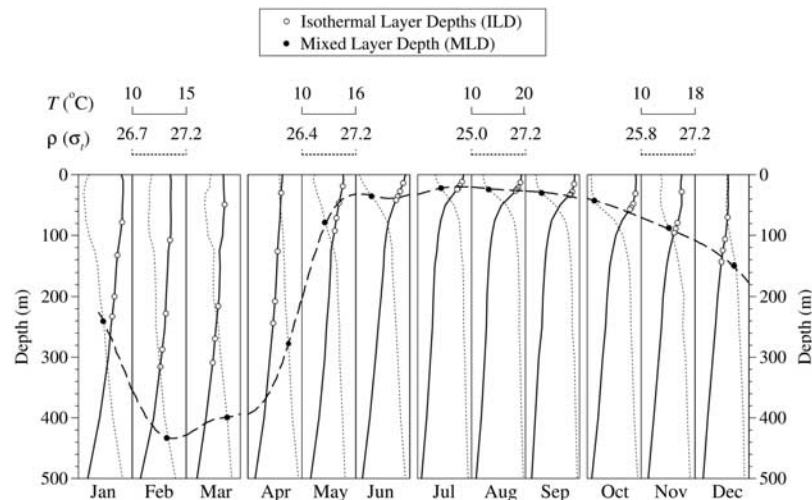
**Figure 2.** Monthly averaged temperature ($T$) and density ($\rho$) profiles constructed from the Levitus data at (45°N, 30°W) in the North Atlantic. The mixed layer depth (MLD) is obtained using a 0.8°C temperature difference and includes the effect of salinity. The MLD is shown with a solid circle on the density profile of each month. Similarly, isothermal layer depths (ILDs) based solely on a temperature change from the surface of $\Delta T = 0.1°$, $0.5°$, $0.8°$, and $1.0°$C are shown by open circles on the temperature profiles. The dashed line highlights the annual cycle of MLD.

the previous section. Letting $T$ denote temperature, the ILD can be summarized in its simplest form as being the depth at the base of an isothermal layer, where the temperature has changed by a fixed amount of $\Delta T$ from the temperature at a reference depth of 10 m. Similarly, letting $S$ denote salinity, and $P$ pressure, the MLD is the depth at the base of an isopycnal layer where the density has changed by a fixed amount of $\Delta\sigma_t = \sigma_t(T + \Delta T, S, P) - \sigma_t(T, S, P)$, where $P = 0$, from the density at a reference depth of 10 m. Note that our $\Delta\sigma_t$ criterion varies based on a fixed $\Delta T$, and this differs from the variable density criterion of $\Delta\sigma_t = (\partial\sigma_t/\partial T)\,\Delta T$ used by *Monterey and Levitus* [1997] in their study of ILD and MLD. Their choice was motivated by a desire to express density change in terms of a coefficient of thermal expansion. Our fields differ from those of *Monterey and Levitus* [1997] in both the defining criteria and the method applied to infer the layer depth. As a consequence, the ILD and MLD fields derived using our methodology are generally deeper than those obtained by theirs for two major reasons: our larger temperature difference criterion of 0.8°C versus their choice of 0.5°C, and the implementation of our simple convective mixing scheme to remove instabilities from density profiles.

[19] The implementation of our criteria requires a multi-step procedure that is separately applied when determining an ILD or MLD. This procedure is described in detail by *Kara et al.* [2000a]. So only the basic characteristics are discussed here. Both the ILD and MLD are defined by a $\Delta T$ criterion, as the $\Delta\sigma_t$ is derived from a $\Delta T$ in the case of MLD. This approach has the advantage of allowing ILD and MLD comparisons, where the $\Delta\sigma_t$ for a MLD is related to the same $\Delta T$ used in defining an ILD, while allowing either $\Delta T$ or $\Delta\sigma_t$ to determine the depth of mixing as appropriate. We note the latter does give a bias toward MLD relative to ILD (typically MLD < ILD) when both temperature and salinity participate in the determination of MLD. This bias slightly increases as the $\Delta T$ criterion increases, with the bias being toward shallower (deeper) values when the salinity

increases (decreases) with depth above the MLD [*Kara et al.*, 2000b].

[20] The methodology we apply here accommodates the wide variety of density and temperature stratifications found in the global ocean: a subsurface mixed layer underlying a surface thermal inversion; multiple fossil layers beneath the surface mixed layer; dicothermal layer (i.e., "a layer of cold water, down to −1.6°C, sandwiched between the warmer surface and deeper layers" [*Pickard and Emery*, 1990, p. 40]); as well as the typical temperature profiles with strong and weak thermoclines found in the middle and low latitudes of the global ocean. For example, water in subpolar regions is nearly isothermal for the Northern and Southern Hemispheres. This results in a MLD that is shallower than the ILD because a shallower halocline is also present. Furthermore, salinity is relatively important in determining the density of seawater at temperatures near freezing as occurs in the subpolar regions. The density difference ($\Delta\sigma_t$) in our variable density criterion is an attempt to reflect the true surface layer depth.

[21] Figure 2 shows an example of monthly MLD and ILD values obtained using our methodology for the location (45°N, 30°W) in the North Atlantic Ocean. In general, the North Atlantic Ocean is one of the ocean regions where deep mixed layer formation is expected in winter [e.g., *Kelly*, 1994; *Tang et al.*, 1999]. As expected, the ILD deepens as $\Delta T$ increases from 0.1°C to 1.0°C. The importance of including salinity is evident when determining the MLD at this particular location. Overall, the MLD is seen to more closely delineate the winter deepening of the mixed layer indicated by the density profiles than any of the ILD for any $\Delta T$ definition. The differences between MLD and ILD values in summer months are usually small.

## 4. Overview of Global MLD Variability

[22] In this section we examine spatial and temporal characteristics of MLD over the global ocean extending
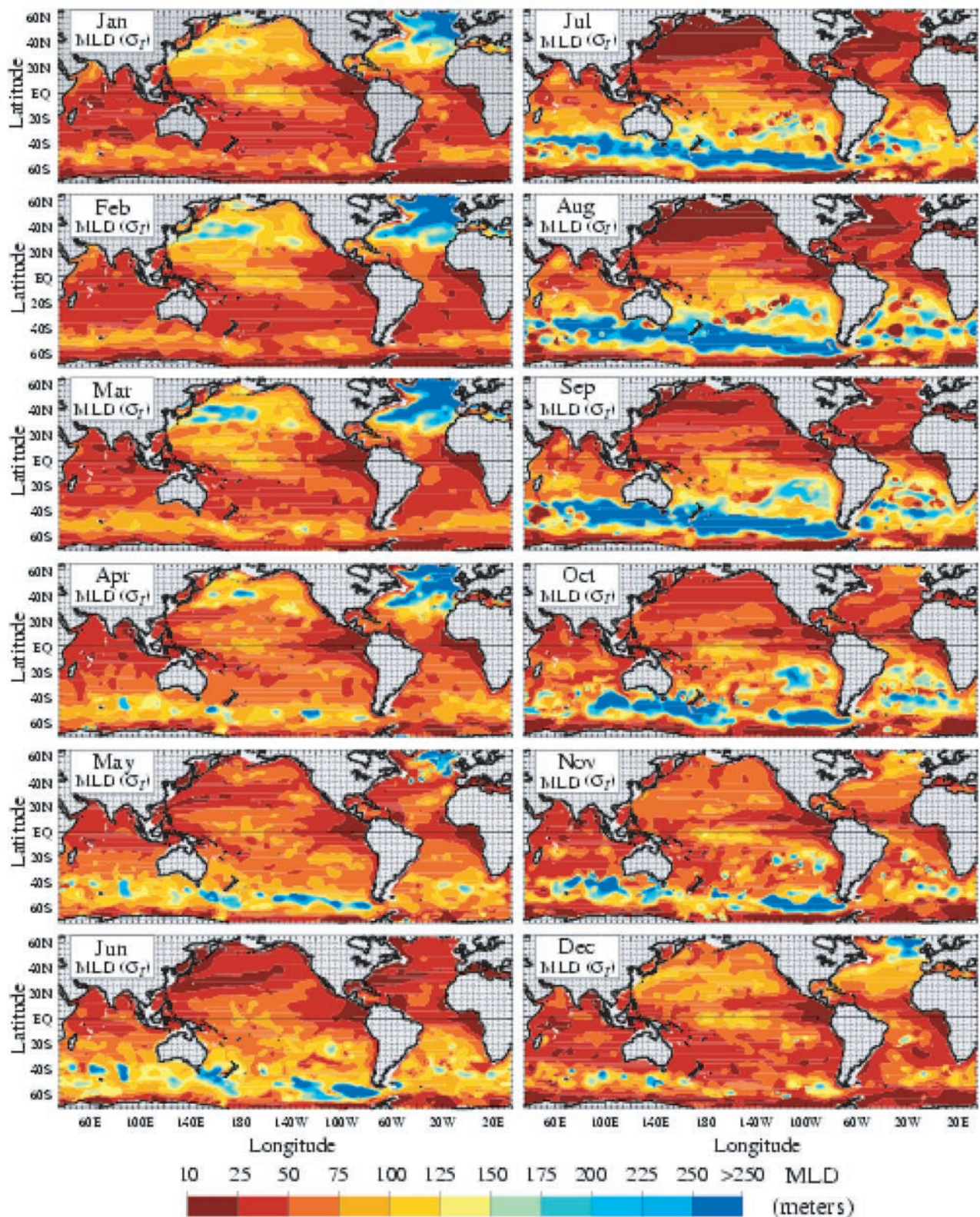
**Figure 3.** Climatological mean mixed layer depth (MLD) fields defined using the density-based criterion with $\Delta T = 0.8°C$.

from 72°S to 65°N. The MLD definition, which includes salinity effects that were summarized in Section 3, is applied to the Levitus data to obtain the surface MLD fields for each month. We follow *Levitus and Boyer* [1994] in our definition of the Northern Hemisphere seasons: January, February, and March (winter); April, May, and June (spring); July, August, and September (summer); and October, November, and December (fall).
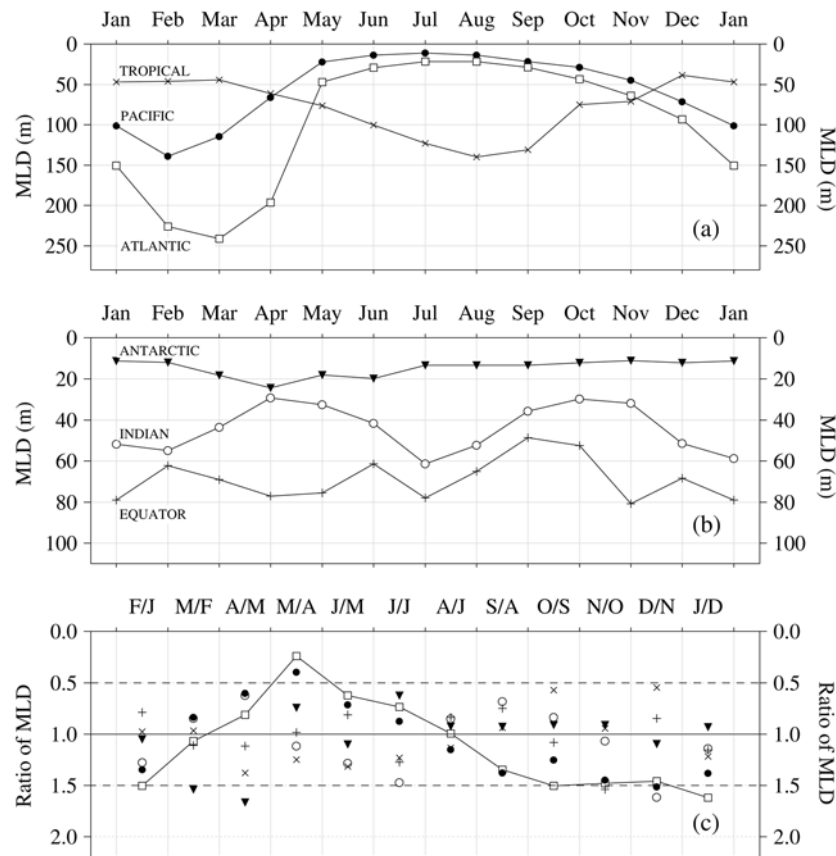
**Figure 4.** Annual changes of mixed layer depth (MLD) at selected locations in the global ocean: (a) Tropical Ocean (20°S, 140°W), Pacific Ocean (30°N, 160°E), and Atlantic Ocean (40°N, 30°W); (b) Antarctic (70°S, 100°W), Indian Ocean (10°N, 55°E), and Equator (1°S, 170°E); and (c) the ratio of two MLD between two consecutive months. The symbols in Figure 4c correspond with those in Figures 4a and 4b. On the x axis, F/J, for example, denotes the MLD increase from January to February (i.e., MLD value in February divided by MLD value in January).

[23] Figure 3 shows the MLD fields over the global ocean by month, separately. The most obvious characteristic is the shallow mixed layer in summer versus a deep one in winter in each hemisphere. The shallow summer mixed layers are consistent with summer heating of the upper ocean along with relatively weak winds, while the deep winter mixed layers are generated by winter cooling and stronger winds. The well known feature of deep mixed layers in the North Pacific and North Atlantic in winter are evident, with the deepest MLD in the North Atlantic Ocean occurring in the region of deep water formation poleward of 40°N from January through May. The MLD in these regions become much shallower in spring, with the region of deepest MLD occurring progressively further north and then disappearing. The regions of deep MLD reappear again in the fall to subsequently reach their maximum depth in winter.

[24] The wintertime mixed layer in the subpolar North Pacific does not deepen as much as in the Atlantic because of a barrier layer formed by a halocline that is maintained by precipitation and slow upwelling from below [Kara et al., 2000b]. Using eddy-resolving XBT data, Sprintall and Roemmich [1999] showed that fossil layers are predomi-

nantly a springtime feature, and are associated with regions of Subtropical Mode Water formation in the southwest Pacific and northeast Pacific Ocean. In the strong western boundary current regions of the Kuroshio and Gulf Stream the MLD is at its deepest in winter and then shallows dramatically by summer. The Indian Ocean is dominated by two periods of strong winds during the year (i.e., the northeast and southwest monsoons). This strong seasonal variability in the surface winds and related sensible and latent heat fluxes dominate in determining the Indian Ocean MLD, especially in the Arabian Sea [e.g., Bauer et al., 1991].

[25] For the MLD fields at the equatorial ocean a minimum MLD tongue is found to be centered in the eastern equatorial Pacific during the Northern Hemisphere winter. Lukas and Lindstrom [1991] and Delcroix et al. [1992] have previously explained the importance of salinity stratification in determining the MLD in the western equatorial Pacific due to the existence of a barrier layer. Roemmich et al. [1994] suggested that barrier layers can be created when fresher surface water from the west flows eastward over the central Pacific water in an equatorial surface jet. Note that the general zonal character of troughs and ridges in the
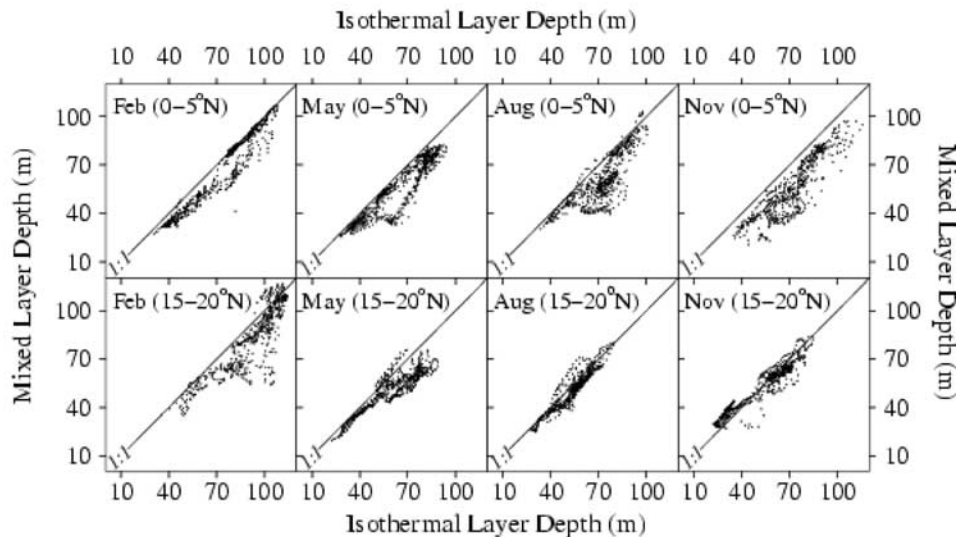
**Figure 5.** Prediction of ILD by MLD at the equatorial ocean and away from the Equator for the midmonths of winter, spring, summer, and fall, respectively. All ILD and MLD values are obtained at each $1° \times 1°$ grid point for the given latitude belt. For both ILD and MLD a $\Delta T$ value of $0.8°C$ is used.

tropical MLD are related to the presence of equatorial current-countercurrent systems [*Bathen*, 1972]. The region between 40°S–60°S in the Southern Hemisphere is characterized by deep mixed layers that span a large zonal region over the globe. The shallowest MLD occurs in the Antarctic below 60°S and is less than 25 m mainly due to fresh water flux from the Antarctic Continent [e.g., *Parkinson*, 1991; *Rintoul et al.*, 1997].

[26] To obtain a general picture of monthly MLD variability we examine the annual depth cycle of the surface mixed layer for selected regions of the global ocean (Figure 4). There is a typical winter deepening and summer shallowing in the North Pacific, Atlantic and most of the Southern Ocean, while the MLD for the Indian Ocean exhibits a semiannual cycle because of the combination of monsoon winds and solar heating. The latter feature has been noted previously by *Monterey and Levitus* [1997]. An indication of the fractional magnitude of the seasonal MLD variability can also be obtained by looking at the maximum and minimum ratio of the MLD between two consecutive months. The ratios in these examples show the largest fractional change in MLD between two consecutive months occurs in the Antarctic from March to April, albeit the change in MLD itself is relatively small.

## 5. ILD and MLD Correspondence

[27] While the ILD is generally coincident with the MLD over most of the global ocean because of the presence of a very strong thermocline, there are regions such as the southern latitudes where there are large differences between the ILD and MLD. In the particular case of high southern latitudes stable water columns can occur despite sharp temperature inversions because of the compensating effect of the salinity [*Gloersen and Campbell*, 1988]. This occurs because the thermal expansion coefficient is very small in this region, thereby allowing salinity variability to become relatively important. For other regions a small temperature

difference corresponds to a relatively large density change because of the nonlinear dependence of the thermal expansion coefficient on temperature [e.g., *Gill*, 1982; *Webster*, 1994]. For this reason the ILD defined using a given $\Delta T$ criterion will not be coincident with the MLD defined using a density difference criterion based on the same $\Delta T$ value, with the ILD usually being shallower than the MLD. To have an ILD that is coincident with the MLD it would be necessary to use a larger $\Delta T$ value for the ILD definition. Given the common use of ILD as the indication of MLD in the literature [e.g., *Lamb*, 1984; *Martin*, 1985], it is worthwhile to ask what $\Delta T$ defined ILD corresponds best to our optimal definition of MLD. This would help to assess the accuracy of the MLD determination in those instances where an ILD definition was applied. It would also be of benefit in those situations where only temperature data with depth are available because salinity measurements with depth are not as common as those for temperature.

[28] Large differences between the $\Delta T$ value for the ILD and the $0.8°C$ criterion used for the MLD can occur where the halocline is shallower than the thermocline, a common occurrence in the western equatorial Pacific and at high latitudes. Another reason for depth differences is that when the same $\Delta T$ criterion is used for both ILD and MLD, strong salinity variations with depth can cause the MLD to be deeper than the ILD (Figure 2), or shallower than the ILD, depending on the sign of the salinity gradient with depth. Still another reason is that oceanic density is more sensitive to temperature changes in some regions, while being more sensitive to salinity in others because of the strong temperature dependence of the coefficient of thermal expansion [e.g., *Gill*, 1982]. For example, it has been explained how the tropical oceans are controlled by factors that change temperature, such as net heat flux and freshwater fluxes due to precipitation [*Webster*, 1994], while also being influenced by factors that change salinity, such as evaporation minus precipitation and river runoff [*Chahine*, 1992]. An example of the differences between the ILD and MLD is shown in
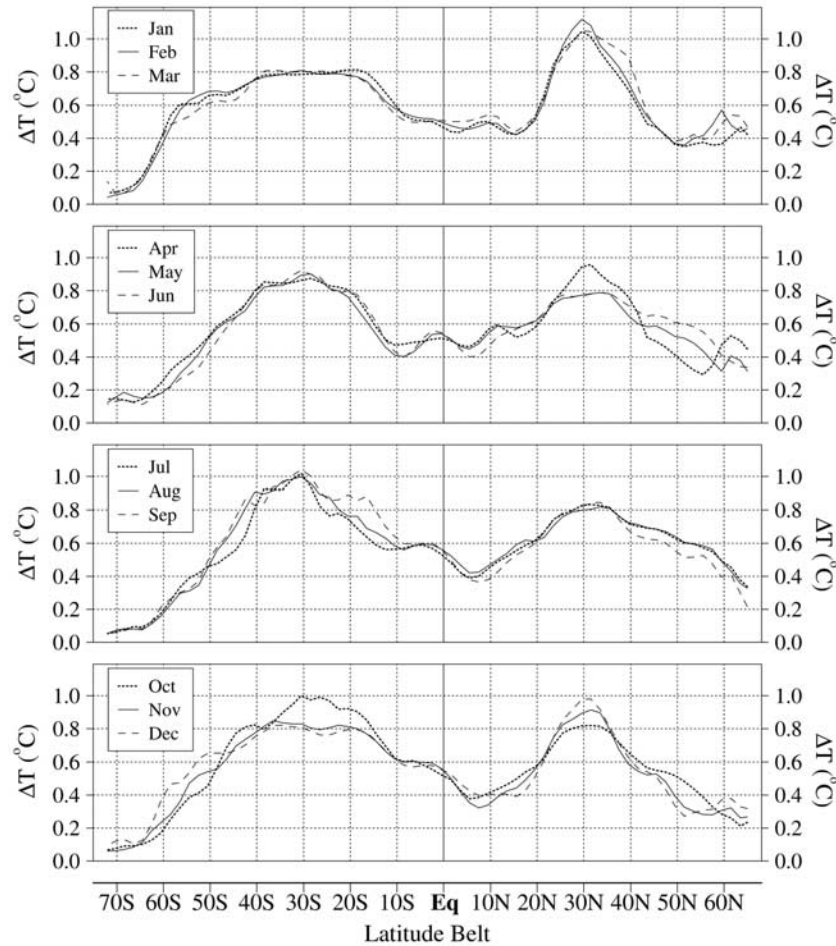
**Figure 6.** The values of $\Delta T$ over the global ocean that best give an ILD corresponding to MLD (based on a $\sigma_t$ with $\Delta T = 0.8°C$ using the methodology of *Kara et al.* [2000a]). The $\Delta T$ values are zonally averaged at each 1° latitude band from 72°S to 65°N. The analysis is shown for each month separately: (a) January, February, and March; (b) April, May, and June; (c) July, August, and September; and (d) October, November, and December.

Figure 5, which clearly shows an ILD can yield very different results when used as a substitute for MLD. This difference is especially evident at 0–5°N in comparison to 15–20°N.

[29] To determine the $\Delta T$ defined ILD that most closely matches the MLD, we use the global monthly fields of ILD and MLD from the NMLD climatologies [*Kara et al.*, 2002]. The value of $\Delta T$ that yields an ILD equal to the

**Table 1.** Zonally Averaged $\Delta T$ Statistics[a]

| | Global Ocean | | | | Equatorial Ocean | | | |
|---|---|---|---|---|---|---|---|---|
| Month | Mean | Standard Deviation | Minimum | Maximum | Mean | Standard Deviation | Minimum | Maximum |
| January | 0.58 | 0.22 | 0.07 | 1.04 | 0.50 | 0.05 | 0.44 | 0.61 |
| February | 0.59 | 0.23 | 0.04 | 1.12 | 0.50 | 0.04 | 0.46 | 0.58 |
| March | 0.59 | 0.22 | 0.07 | 1.05 | 0.51 | 0.02 | 0.50 | 0.55 |
| April | 0.57 | 0.22 | 0.13 | 0.96 | 0.49 | 0.03 | 0.46 | 0.56 |
| May | 0.55 | 0.20 | 0.12 | 0.90 | 0.48 | 0.05 | 0.40 | 0.54 |
| June | 0.56 | 0.22 | 0.11 | 0.92 | 0.46 | 0.05 | 0.39 | 0.56 |
| July | 0.58 | 0.23 | 0.05 | 1.02 | 0.50 | 0.07 | 0.39 | 0.59 |
| August | 0.59 | 0.24 | 0.05 | 0.99 | 0.53 | 0.06 | 0.42 | 0.59 |
| September | 0.58 | 0.25 | 0.05 | 1.04 | 0.51 | 0.10 | 0.37 | 0.64 |
| October | 0.58 | 0.26 | 0.07 | 0.99 | 0.51 | 0.09 | 0.38 | 0.62 |
| November | 0.54 | 0.24 | 0.06 | 0.91 | 0.50 | 0.11 | 0.32 | 0.61 |
| December | 0.56 | 0.22 | 0.09 | 0.98 | 0.52 | 0.08 | 0.40 | 0.62 |

[a]All values are in °C. Global ocean is defined as the latitude belts between 72°S to 65°N and the equatorial Ocean is defined as between 10°S to 10°N.
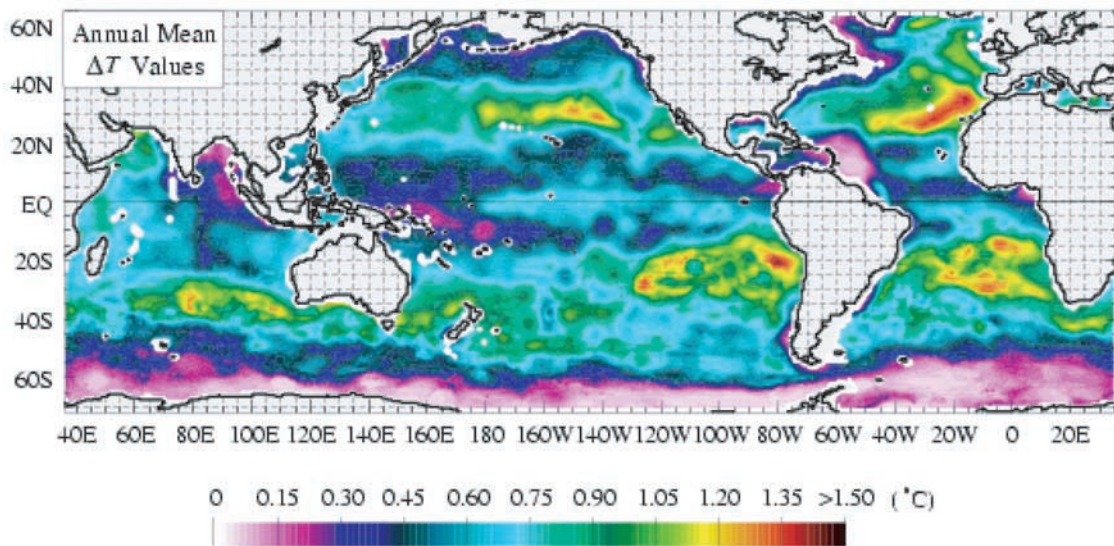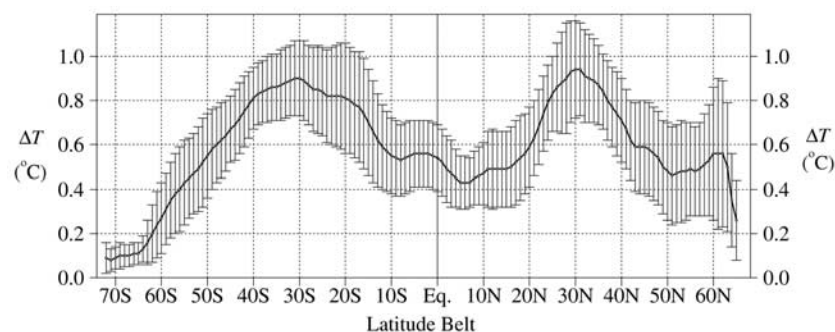
**Figure 7.** The annual average of the $\Delta T$ values (see Figure 6) that best give an ILD corresponding to MLD (based on $\sigma_t$ with $\Delta T = 0.8°C$) over the global ocean. The value of $\Delta T$ for which the ILD equals the MLD is determined at each $1° \times 1°$ box by applying a linear regression using the ILD ($\Delta T$) for the $\Delta T$ values from 0.1 to 1.5°C.

MLD (i.e., for a $\Delta\sigma_t$ with $\Delta T = 0.8°C$) is determined at each ocean grid point ($1° \times 1°$ boxes) by applying a linear regression using the ILD($\Delta T$) for the $\Delta T$ values of 0.1, 0.2., 0.3, 0.5, 0.8, 1.0, 1.2 and 1.5°C. This is done for each month from January to December (Figure 6). Presented in Table 1 are the zonally averaged mean, standard deviation, minimum and maximum $\Delta T$ values for which the surface ocean layer depth obtained from the ILD corresponds to the MLD. During the Northern Hemisphere winter an ILD($\Delta T$) of $\Delta T \geq 1°C$ is required to obtain the optimal MLD near 30°N. The annual mean of the calculated $\Delta T$ values is presented in Figure 7. Over a global ocean average, a $\Delta T$ value of 0.6°C for ILD best approximates the MLD (based on $\sigma_t$ with $\Delta T = 0.8°C$) but with substantial seasonal and regional variation as discussed. For the Antarctic Ocean the $\Delta T$ values are substantially less than 0.6°C as this is also evident from the annual mean $\Delta T$ values (Figure 8). The North Atlantic Ocean generally shows large $\Delta T$ values (especially during winter). The $\Delta T$ values do not change significantly in the equatorial ocean, having an annual mean value of approximately 0.5°C. In general, the high southern latitudes and equatorial regions require $\Delta T$ values as low as 0.1 and 0.4°C, respectively, regardless of the month. This reveals the influence of the strong salinity stratification on the MLD determination for these regions.

## 6. Validation of ILD Versus MLD Correspondence

[30] To validate the ILD versus MLD correspondence we use daily averaged subsurface temperature and salinity data obtained from selected moorings in the global ocean. From the overview presented in Section 4, two particular areas of interest are the western equatorial Pacific warm pool where salinity stratification is known to be important, and the Arabian Sea where there is strong seasonal variability in the surface winds. For the former there are mooring data available from the Tropical Atmosphere



**Figure 8.** The annual average of the $\Delta T$ values (see Figure 5) that best give an ILD corresponding to the MLD. Also included are the ± standard deviations for the zonally averaged annual $\Delta T$ values.
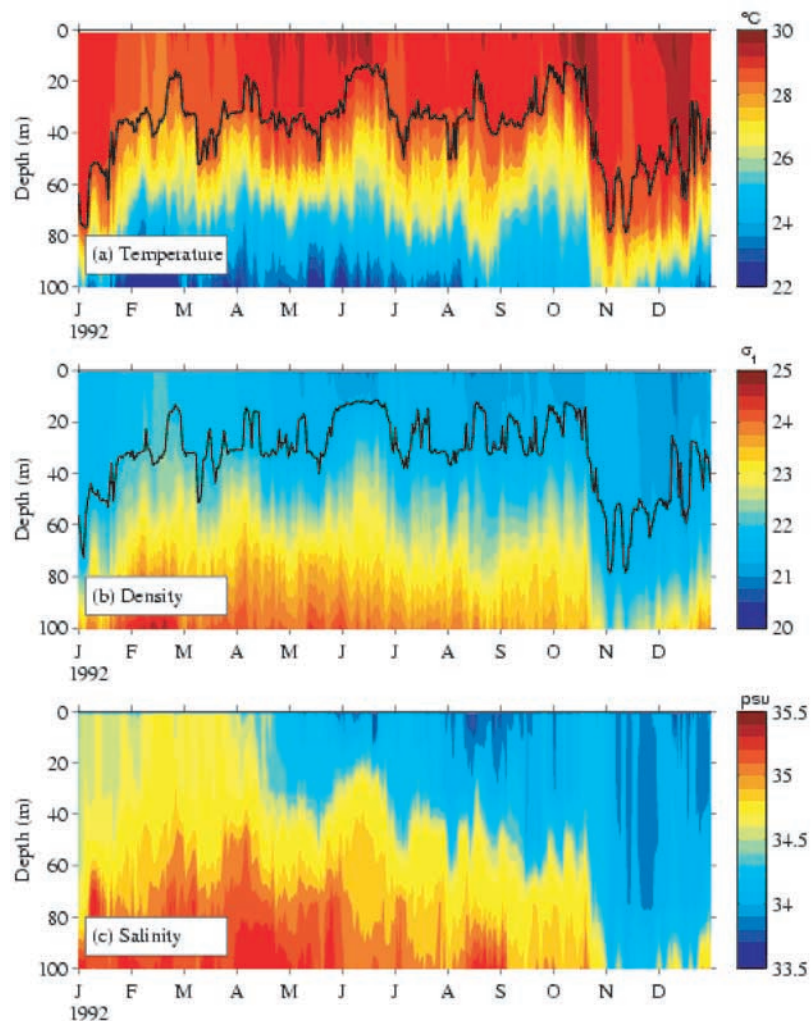
**Figure 9.** Daily averaged observational subsurface temperature and salinity variability and computed density down to the 150 m depth at (0°N, 156°E) in the western equatorial Pacific warm pool in 1992: (a) subsurface temperatures and ILD (0.3°C) calculated from the temperature-based layer depth definition, (b) density and MLD (0.8°C) calculated from the density-based layer depth definition (i.e., optimal MLD), and (c) salinities. Note that the temperatures are accurate to about 0.03°C [*Freitag et al.*, 1994] and the salinities are accurate to about 0.02 psu [*Freitag et al.*, 1999].

Ocean (TAO) Array [*McPhaden*, 1995], while for the latter there are data from a Woods Hole Oceanographic Institute (WHOI) mooring in the central Arabian Sea [*Weller et al.*, 1998].

[31] The TAO mooring at (0°N, 156°E) in the western equatorial Pacific warm pool is chosen because it has contemporaneous subsurface temperature and salinity data for 1992 that has sufficiently high vertical resolution and almost no data voids. The subsurface data are daily averages of 10 minute sampled data at 8 discrete depths of 1, 10, 30, 50, 75, 100, 150, and 200 m. There were only some periods when subsurface temperature and salinity measurements from the buoys were not available. These mostly occurred at depths greater than 300 m and were filled in using a cubic spline. This substitution did not affect the results because the ILD or MLD in the equatorial ocean is usually less than 150 m. The density is calculated using the UNESCO equation of state with no pressure dependence so that the

MLD can be determined using our method. At this location a $\Delta T$ value of $\approx 0.3$°C (see Figure 7) is required to obtain a ILD that corresponds to our optimal MLD.

[32] The daily ILD (0.3°C) variability as well as the daily MLD variability at (0°N, 156°E) are shown in Figure 9. The ILD shown for $\Delta T = 0.3$°C is almost equal to the MLD. This is made further evident by also comparing the ILD obtained using larger $\Delta T$ values of 0.8 and 1.2°C (Figure 10). For this particular location the correspondence derived based on the annual mean $\Delta T$ field works very well.

[33] To investigate the error bounds when using an incorrect ILD to represent the MLD we consider several statistical metrics together when applied to the ILDs determined using $\Delta T$ values of 0.2, 0.3, 0.5, 0.8, 1.0, 1.2 and 1.5°C. Let $X_i$ ($i = 1, 2, \ldots, n$) be the set of $n$ reference values (i.e., MLD values), and let $Y_i$ ($i = 1, 2, \ldots, n$) be the set of estimates (i.e., ILD values). Also let $\bar{X}$ ($\bar{Y}$) and $\sigma_X$ ($\sigma_Y$) be
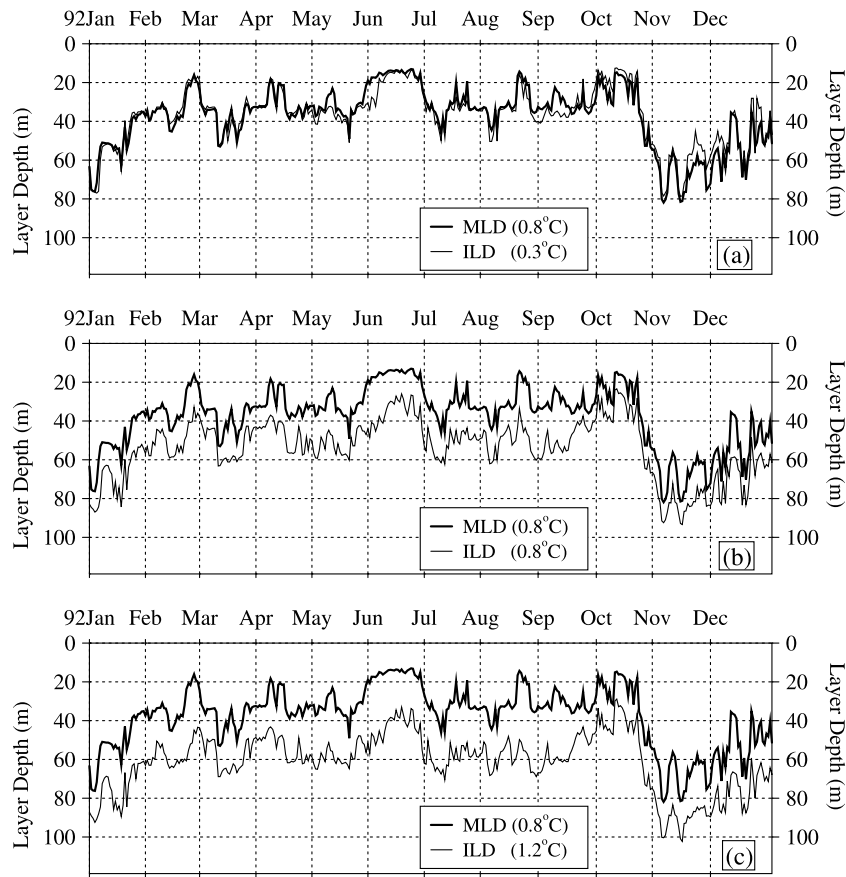
**Figure 10.** Comparisons of daily time series ocean layer depths between MLD and ILD at (0°N, 156°E) in the western equatorial Pacific warm pool in 1992: (a) MLD (0.8°C) versus ILD (0.3°C), (b) MLD (0.8°C) versus ILD (0.8°C), and (c) MLD (0.8°C) versus ILD (1.2°C).

the mean and standard deviations of the reference (estimate) values, respectively. For the 1992 time series of daily TAO mooring data used here $n = 366$. Following *Murphy* [1988] the statistical relationships between optimal MLD ($X$) and ILD ($Y$) values can therefore be expressed as

$$ME = \bar{Y} - \bar{X}, \tag{1}$$

$$RMS = \left[ \frac{1}{n} \sum_{i=1}^{n} (Y_i - X_i)^2 \right]^{1/2}, \tag{2}$$

$$R = \frac{1}{n} \sum_{i=1}^{n} (X_i - \bar{X})(Y_i - \bar{Y}) / (\sigma_X \sigma_Y), \tag{3}$$

$$SS = 1 - \frac{RMS^2}{\sigma_X^2}, \tag{4}$$

where ME is the bias or annual mean difference, RMS is root mean square difference, $R$ is correlation coefficient, and SS is the skill score. The SS is 1.0 for an ILD time series that corresponds perfectly to the MLD, and positive skill is usually considered to represent a minimal level of acceptable performance [*Murphy and Epstein*, 1989].

[34] As seen from Table 2, the smallest RMS and ME values are obtained for ILD(0.3°C). This is also evident from the latter having the highest SS value of 0.91 in comparison to the ILDs. The negative SS values for both ILD(1.2°C) and ILD(1.5°C) indicate a poor overlap with the MLD. While the SS values for ILD(0.2°C) and ILD(0.5°C) are large and positive (0.82 and 0.81, respectively) we note their RMS differences and ME values are large in comparison to those for ILD(0.3°C). For all $\Delta T$ values used in the

**Table 2.** Optimal MLD(0.8°C) Versus ILD at (0°N, 156°E)[a]

| Layer Depth Comparisons | RMS, m | ME, m | R | SS |
|---|---|---|---|---|
| MLD(0.8°C) versus ILD(0.2°C) | 6.6 | −2.8 | 0.92 | 0.82 |
| MLD(0.8°C) versus ILD(0.3°C) | 4.8 | 0.5 | 0.95 | 0.91 |
| MLD(0.8°C) versus ILD(0.5°C) | 6.9 | 5.2 | 0.96 | 0.81 |
| MLD(0.8°C) versus ILD(0.8°C) | 11.7 | 10.5 | 0.95 | 0.44 |
| MLD(0.8°C) versus ILD(1.0°C) | 14.4 | 13.4 | 0.94 | 0.14 |
| MLD(0.8°C) versus ILD(1.2°C) | 16.9 | 15.9 | 0.93 | −0.18 |
| MLD(0.8°C) versus ILD(1.5°C) | 20.9 | 19.4 | 0.92 | −0.72 |

[a]The ILD and MLD comparisons obtained from the daily averaged TAO subsurface temperature and salinity measurements in 1992. Monthly mean $\Delta T$ values for January through December are 0.28°, 0.28°, 0.30°, 0.33°, 0.34°, 0.20°, 0.16°, 0.30°, 0.18°, 0.31°, 0.32°, and 0.27°C. All statistics for each category are based on the 366 daily averaged layer depth values.
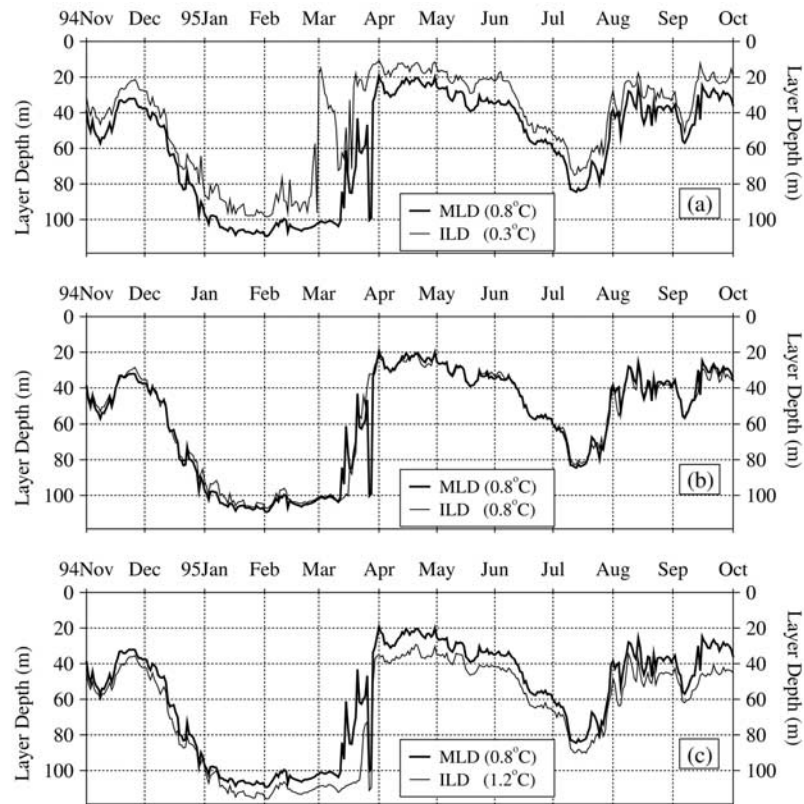
**Figure 11.** Same as Figure 10 but at (15.5°N, 61.5°E) in the Arabian Sea of the Indian Ocean from November 1994 to October 1995: (a) MLD (0.8°C) versus ILD (0.3°C), (b) MLD (0.8°C) versus ILD (0.8°C), and (c) MLD (0.8°C) versus ILD (1.2°C).

ILD definition we obtain large $R$ values greater than 0.90, indicating our methodology for MLD determination is able to reproduce the seasonal cycle well.

[35] As the second validation test we use data from the WHOI mooring at (15.5°N, 61.5°E) in the central Arabian Sea. This mooring has almost a continuous time series of subsurface temperature and salinity data sampled at a high-frequency interval of 7.5 minutes or less that spans 1 November 1994 to 30 September 1995. The availability of this data makes this an ideal source with which to verify ILD versus MLD in a region where the salinity stratification is not as important as in the equatorial warm pool, and where a strong seasonal variation in MLD occurs because of strong and seasonally reversing monsoon winds. The MLD and ILDs are calculated using daily averaged data as in the case of the TAO mooring above and the same statistical measures are determined. Deepening of the MLD is evident during both the winter (1 November 1994 to 15 February 1995) and summer (1 June 1995 to 15 September 1995) monsoon periods (Figure 11). The ILD(0.8°C) is in best agreement with the MLD, with the ILD obtained using larger temperature difference criteria being markedly deeper. For the value of ≈0.8°C obtained from the annual mean $\Delta T$ field at this location (see Figure 7) the ILD(0.8°C) has the smallest ME of −0.8 m and RMS difference of 6.6 m (Table 3). While the statistics for ILD(1.0°C) and ILD(0.8°C) are similar to each other, the latter has a slightly larger ME value of 2.1 m. Note that the best SS value occurs for ILD(0.8°C) and

ILD(1.0°C). While positive and large SS values are evident for all ILDs the RMS differences and ME values are the lowest for ILD(0.8°C) and ILD(1.0°C).

## 7. Conclusions

[36] We have presented monthly climatological fields of surface ocean mixed layer depth for the global ocean. The criterion we used to define MLD is based on water density, and thereby takes into account the effects of both temperature and salinity. We have also created a set of ILD climatologies with different $\Delta T$ criteria because: 1) having both MLD and ILD is useful in the study of barrier layers, and 2) it is sometimes necessary due to salinity data limitations to use an ILD in place of MLD. Because these MLD and ILD fields are obtained from 1° resolution climatologies of temperature and salinity for the global ocean, we have elaborated upon the limitations of the temperature and salinity data used, as well as the modifications applied to overcome them in determining the MLD and ILD. Using these seasonal and monthly MLD climatologies we have shown the strong seasonality of MLD in middle to high latitudes and very shallow MLD at high latitudes.

[37] A comparison of the ILD with the MLD was made to determine an ILD definition that is most nearly equivalent to our optimal MLD. While this ILD definition does vary with space and time, we have found a $\Delta T$ of 0.6°C for the

**Table 3.** Optimal MLD(0.8°C) Versus ILD at (15.5°N, 61.5°E)[a]

| Layer Depth Comparisons | RMS, m | ME, m | $R$ | SS |
|---|---|---|---|---|
| MLD(0.8°C) versus ILD(0.2°C) | 22.9 | −14.5 | 0.80 | 0.39 |
| MLD(0.8°C) versus ILD(0.3°C) | 16.6 | −9.9 | 0.89 | 0.68 |
| MLD(0.8°C) versus ILD(0.5°C) | 11.0 | −5.4 | 0.94 | 0.86 |
| MLD(0.8°C) versus ILD(0.8°C) | 6.6 | −0.8 | 0.97 | 0.95 |
| MLD(0.8°C) versus ILD(1.0°C) | 6.4 | 2.1 | 0.98 | 0.95 |
| MLD(0.8°C) versus ILD(1.2°C) | 7.4 | 3.9 | 0.98 | 0.94 |
| MLD(0.8°C) versus ILD(1.5°C) | 13.2 | 7.2 | 0.93 | 0.80 |

[a]The ILD and MLD comparisons obtained from the daily averaged WHOI subsurface temperature and salinity measurements from November 1994 to October 1995. Monthly mean $\Delta T$ values are 0.86°, 0.81°, 0.64°, 0.89°, 0.91°, 0.83°, 0.82°, 0.88°, 0.79°, 0.70°, 0.82°, and 0.67°C. All statistics for each category are based on the 335 daily averaged layer depth values.

ILD definition yields an ILD that is approximately equal to the MLD over the most of the global ocean. The greatest exception is the Antarctic Ocean where significantly smaller $\Delta T$ values are required. We demonstrated the validity of the ILD correspondence to MLD using subsurface temperature and salinity data from two moorings. One of these moorings is from the Tropical Atmosphere Ocean (TAO) array, and it is located in the western equatorial Pacific warm pool. The other is the Woods Hole Oceanographic Institute (WHOI) mooring deployed in the Arabian Sea from November 1994 to October 1995. Analysis of daily layer depth values obtained from their subsurface data using different $\Delta T$ values showed that the ILDs with $\Delta T$ of 0.3°C and 0.8°C yield an equivalent optimal MLD in the warm pool and Arabian Sea, respectively. These $\Delta T$ values are consistent with the ones drived from the annual mean $\Delta T$. When using the appropriate $\Delta T$ value to define ILD, the correspondence between ILD and MLD for these particular moorings was shown to work very well, with mean errors of ≈1 m between the ILD and the optimal MLD. This enables a good estimate of the MLD to be determined from in situ mooring observations that very frequently do not have salinity data.

[38] Finally, one of our main purposes was to illustrate the value of the global fields of the Naval Research Laboratory Ocean Mixed Layer Depth (NMLD) climatology. It should be kept in mind that limitations still exist for MLD fields because of the inadequate salinity and temperature data in some regions such as much of the Southern Ocean. We used techniques to reduce these limitations and thus provide the most accurate MLD fields we could in these regions of the global ocean. The MLD and ILD fields discussed in this paper are readily available as 1° global monthly, seasonal, and annual means, and are useful for a wide variety of applications as outlined here, including biological modeling, ocean mixed layer model development and evaluation. The MLD and ILD data sets and the algorithm to generate the layer depths are publicly available at the official NRL Stennis Space Center web page, http://www7320.nrlssc.navy.mil/nmld/nmld.html.

## References

Bathen, K. H., On the seasonal changes in the depth of the mixed layer in the North Pacific Ocean, *J. Geophys. Res.*, *77*, 7138−7150, 1972.

Bauer, S., G. L. Hitchcock, and D. B. Olson, Influence of monsoonally-forced Ekman dynamics upon surface layer depth and plankton biomass distribution in the Arabian Sea, *Deep Sea Res., Part I*, *38*, 531−553, 1991.

Bretherton, F. P., M. J. McPhaden, and E. B. Kraus, Design studies for climatological measurements of heat storage, *J. Phys. Oceanogr.*, *14*, 318−337, 1984.

Chahine, M. T., The hydrological cycle and its influence on climate, *Nature*, *359*, 373−380, 1992.

Chen, D., A. J. Busalacchi, and L. M. Rothstein, The roles of vertical mixing, solar radiation, and wind stress in a model simulation of the sea surface temperature seasonal cycle in the tropical Pacific Ocean, *J. Geophys. Res.*, *99*, 20,345−20,359, 1994.

Cherniawsky, J., and G. Holloway, An upper-ocean general circulation model for the North Pacific: Preliminary experiments, *Atmos. Ocean*, *29*, 737−784, 1991.

Colossi, J., and T. P. Barnett, The characteristic spatial and temporal scales for SLP, SST, and air temperature in the Southern Hemisphere, *J. Appl. Meteorol.*, *29*, 694−703, 1990.

Delcroix, T., G. Eldin, M.-H. Radenac, J. Toole, and E. Firing, Variation of the western equatorial Pacific Ocean, *J. Geophys. Res.*, *97*, 5423−5445, 1992.

Fasham, M. J. R., Variations in the seasonal cycle of biological production in subarctic oceans: A model sensitivity analysis, *Deep Sea Res., Part I*, *42*, 1111−1149, 1995.

Festa, J. F., and R. L. Molinari, An evaluation of the WOCE volunteer observing ship XBT network in the Atlantic, *J. Atmos. Oceanic Technol.*, *9*, 305−317, 1992.

Freitag, H. P., Y. Feng, L. J. Mangum, M. J. McPhaden, J. Neander, and L. D. Stratton, Calibration, procedures and instrumental accuracy estimates of TAO temperature, relative humidity and radiation measurements, *NOAA Tech. Memo. ERL PMEL-104*, 32 pp., Natl. Oceanic and Atmos. Admin., Silver Spring, Md., 1994. [Available from Pacific Marine Environmental Laboratory, 7600 Sand Point Way, Seattle, WA 98115, USA.]

Freitag, H. P., M. E. McCarty, C. Nosse, R. Lukas, M. J. McPhaden, and M. F. Cronin, COARE Seacat data: Calibrations and quality control procedures, *NOAA Tech. Memo. ERL PMEL PB99-146144*, 89 pp., Natl. Oceanic and Atmos. Admin., Silver Spring, Md., 1999. (Available from Pac. Mar. Environ. Lab. Seattle, Wash.)

Gill, A. E., *Atmosphere-Ocean Dynamics*, *Int. Geophys. Ser.*, vol. 30, 662 pp., Academic, San Diego, Calif., 1982.

Gloersen, P., and W. J. Campbell, Variations in the Arctic, Antarctic, and global sea ice cover during 1978−1987 as observed with Nimbus-7 SMMR, *J. Geophys. Res.*, *93*, 10,666−10,740, 1988.

Gouretski, V. V., A description and quality assessment of the historical hydrographic data for the South Pacific Ocean, *J. Atmos. Oceanic Technol.*, *16*, 1791−1815, 1999.

Hayes, S. P., L. J. Mangum, J. Picaut, A. Sumi, and K. Takeuchi, TOGA-TAO: A moored array for real-time measurements in the tropical Pacific Ocean, *Bull. Am. Meteorol. Soc.*, *72*, 339−347, 1991.

Kara, A. B., P. A. Rochford, and H. E. Hurlburt, An optimal definition for ocean mixed layer depth, *J. Geophys. Res.*, *105*, 16,803−16,821, 2000a.

Kara, A. B., P. A. Rochford, and H. E. Hurlburt, Mixed layer depth variability and barrier layer formation over the North Pacific Ocean, *J. Geophys. Res.*, *105*, 16,783−16,801, 2000b.

Kara, A. B., P. A. Rochford, and H. E. Hurlburt, Naval Research Laboratory Mixed Layer Depth (NMLD) Climatologies, *NRL Rep. NRL/FR/7330-02-9995*, 26 pp., 2002. (Available from Nav. Res. Lab., Stennis Space Center, Miss.)

Kelly, D. E., Temperature-salinity criterion for inhibition of deep convection, *J. Phys. Oceanogr.*, *24*, 2424−2433, 1994.

Kent, E. C., P. K. Taylor, B. S. Truscott, and J. A. Hopkins, The accuracy of voluntary observing ship's meteorological observations, *J. Atmos. Oceanic Technol.*, *10*, 591−608, 1993.

Kraus, E. B., and J. S. Turner, A one-dimensional model of the seasonal thermocline, II, The general theory and its consequences, *Tellus*, *19*, 98–106, 1967.

Kundu, P. K., *Fluid Mechanics*, 638 pp., Academic, San Diego, Calif., 1990.

Lamb, P. J., On the mixed layer climatology of the North and tropical Atlantic, *Tellus, Ser. A*, *36*, 292–305, 1984.

Levitus, S., Climatological atlas of the world ocean, *NOAA Prof. Pap. 13*, 173 pp., U.S. Govt. Print. Off., Washington, D.C., 1982.

Levitus, S., and T. P. Boyer, *World Ocean Atlas 1994*, vol. 4, *Temperature, NOAA Atlas NESDIS*, vol. 4, 129 pp., Natl. Oceanic and Atmos. Admin., Silver Spring, Md., 1994.

Levitus, S., R. Burgett, and T. P. Boyer, *World Ocean Atlas 1994*, vol. 3, *Salinity, NOAA Atlas NESDIS*, vol. 3, 111 pp., Natl. Oceanic and Atmos. Admin., Silver Spring, Md., 1994.

Lewis, M. R., M. Carr, G. Feldman, W. Esaias, and C. McClain, Influence of penetrating solar radiation on the heat budget of the equatorial Pacific Ocean, *Nature*, *347*, 543–544, 1990.

Lukas, R., and E. Lindstrom, The mixed layer of the western equatorial Pacific Ocean, *J. Geophys. Res.*, *96*, 3343–3357, 1991.

Martin, P. J., Simulation of the mixed layer at OWS November and Papa with several models, *J. Geophys. Res.*, *90*, 903–916, 1985.

McPhaden, M. J., The Tropical Atmosphere Ocean (TAO) array is completed, *Bull. Am. Meteorol. Soc.*, *76*, 739–741, 1995.

Millero, F. J., and A. Poisson, International one-atmosphere equation of state of seawater, *Deep Sea Res., Part I*, *28*, 625–629, 1981.

Millero, F. J., C.-T. Chen, A. Bradshaw, and K. Schleicher, A new high pressure equation of state for seawater, *Deep Sea Res., Part I*, *27*, 255–264, 1980.

Monterey, G., and S. Levitus, *Seasonal Variability of Mixed Layer Depth for the World Ocean, NOAA Atlas NESDIS*, vol. 14, 100 pp., Natl. Oceanic and Atmos. Admin., Silver Spring, Md., 1997.

Murphy, A. H., Skill scores based on the mean square error and their relationships to the correlation coefficient, *Mon. Weather Rev.*, *116*, 2417–2424, 1988.

Murphy, A. H., and E. S. Epstein, Skill scores and correlation coefficients in model verification, *Mon. Weather Rev.*, *117*, 572–581, 1989.

Obata, A., J. Ishizaka, and M. Endoh, Global verification of critical depth theory for phytoplankton bloom with climatological in situ temperature and satellite ocean color data, *J. Geophys. Res.*, *101*, 20,657–20,667, 1996.

Olbers, D., V. V. Gouretski, G. Seiss, and J. Schröeter, *Hydrographic Atlas of the Southern Ocean*, 17 pp and 82 plates, Alfred Wegener Inst., Bremerhaven, Germany, 1992.

Pailler, K., B. Bourlès, and Y. Gouriou, The barrier layer in the western tropical Atlantic Ocean, *J. Geophys. Res.*, *26*, 2069–2072, 1999.

Parkinson, C. L., Interannual variability of monthly Southern Ocean sea ice distribution, *J. Geophys. Res.*, *96*, 4791–4801, 1991.

Pickard, G. L., and W. J. Emery, *Descriptive Physical Oceanography*, 320 pp., Pergamon, Tarrytown, N.Y., 1990.

Polovina, J. J., G. T. Mitchum, and G. T. Evans, Decadal and basin-scale variation in mixed layer depth and the impact on biological production in the central and North Pacific, 1960–88, *Deep Sea Res., Part I*, *42*, 1701–1716, 1995.

Rintoul, S., J. Donguy, and D. Roemmich, Seasonal evolution of upper ocean thermal structure between Tasmania and Antarctica, *Deep Sea Res., Part I*, *44*, 1185–1202, 1997.

Roemmich, D., M. Y. Morris, W. R. Young, and J. R. Donguy, Fresh equatorial jets, *J. Phys. Oceanogr.*, *24*, 540–558, 1994.

Saunders, P., The accuracy of measurements of salinity, oxygen and temperature in the deep ocean, *J. Phys. Oceanogr.*, *16*, 189–195, 1986.

Sprintall, J., and D. Roemmich, Characterizing the structure of the surface layer in the Pacific Ocean, *J. Geophys. Res.*, *104*, 23,297–23,311, 1999.

Sprintall, J., and M. Tomczak, Evidence of the barrier layer in the surface layer of tropics, *J. Geophys. Res.*, *97*, 7305–7316, 1992.

Sutton, P. J., P. F. Worcester, G. Masters, B. D. Cornuelle, and J. F. Lynch, Ocean mixed layers and acoustic pulse propagation in the Greenland Sea, *J. Acoust. Soc. Am.*, *94*, 1517–1526, 1993.

Tabata, S., and W. E. Weichselbaumer, An update statistics of oceanographic data based on hydrographic/STD casts made at stations 1 through 6 along line P during January 1959 through September 1990, *Can. Data Rep. Hydrogr. Ocean Sci.*, *108*, 317 pp., 1992.

Tang, C. L., Q. Gui, and B. M. DeTracey, A modeling study of upper ocean winter processes in the Labrador Sea, *J. Geophys. Res.*, *104*, 23,411–23,425, 1999.

Vialard, J., and P. Delecluse, An OGCM study for the TOGA decade, part II, Barrier-layer formation and variability, *J. Phys. Oceanogr.*, *28*, 1089–1106, 1998.

Webster, P., The role of hydrological processes in tropical ocean-atmosphere interaction, *J. Geophys. Res.*, *32*, 427–476, 1994.

Weller, R. A., M. F. Baumgartner, S. A. Josey, A. S. Fischer, J. C. Kindle, Atmospheric forcing in the Arabian Sea during 1994–1995: Observations and comparisons with climatology models, *Deep Sea Res., Part I*, *45*, 1961–1999, 1998.

Wilkerson, J. C., and M. D. Earle, A study of differences between environmental reports by ships in the Voluntary Observing Program and measurements from NOAA buoys, *J. Geophys. Res.*, *95*, 3373–3385, 1990.

Woodruff, S. D., R. J. Slutz, R. L. Jenne, and P. M. Steurer, A comprehensive ocean-atmosphere data set, *Bull. Am. Meteorol. Soc.*, *68*, 1239–1250, 1987.

You, Y., Salinity variability and its role in the barrier layer formation during TOGA-COARE, *J. Phys. Oceanogr.*, *25*, 2778–2807, 1995.

————————————

H. E. Hurlburt and P. A. Rochford, Oceanography Division, Naval Research Laboratory, Stennis Space Center, MS 39529, USA. (hurlburt@nrlssc.navy.mil; rochford@nrlssc.navy.mil)

A. B. Kara, Center for Ocean-Atmospheric Prediction Studies, Florida State University, Tallahassee, FL 32306, USA. (kara@nrlssc.navy.mil)